Rotational Raman Lidar measurements of atmospheric temperature in the UV

P. Di Girolamo,[1] R. Marchese,[1] D. N. Whiteman,[2] and B. B. Demoz[2]

Received 5 August 2003; revised 30 September 2003; accepted 13 November 2003; published 13 January 2004.

[1] Measurements of atmospheric temperature have been performed by the NASA Scanning Raman Lidar based on the application of the pure rotational Raman (RR) technique. These measurements represent to our knowledge the first successful lidar measurements of temperature using the RR technique in the UV region, where eye-safe concerns are far less stringent than in the visible and IR. While the system configuration was unoptimized for temperature measurements, nevertheless results were achieved that demonstrate the feasibility of the RR technique for meteorological and climatological applications. Based on 90 minutes data averaging, lidar measurements extend up to 23 km, with RMS deviation between lidar and simultaneous radiosondes not exceeding 1.2 K and average bias smaller than 0.5 K. Simulations reveal that the RR technique in the UV has the potential for providing accurate measurements throughout the troposphere, with appreciable improvement with respect to visible systems for daytime operation. *INDEX TERMS:* 0350 Atmospheric Composition and Structure: Pressure, density, and temperature; 3360 Meteorology and Atmospheric Dynamics: Remote sensing; 3394 Meteorology and Atmospheric Dynamics: Instruments and techniques. **Citation:** Di Girolamo, P., R. Marchese, D. N. Whiteman, and B. B. Demoz (2004), Rotational Raman Lidar measurements of atmospheric temperature in the UV, *Geophys. Res. Lett.*, *31*, L01106, doi:10.1029/2003GL018342.

1. Introduction

[2] Understanding of meteorological processes and climate trends requires accurate, high time and space resolution measurements of atmospheric temperature. Specific observational requirements to be fulfilled by networks of ground-based and satellite remote sensors have been defined by the World Meteorological Organization [*WMO*, 1996; *CEOS/WMO Online Database*, 2003], which imply globally distributed measurements of atmospheric temperature throughout the troposphere with an accuracy of 0.5 K and a vertical and temporal resolution of 0.1 km and 15 minutes, respectively.

[3] Lidar systems based on the application of the pure rotational Raman technique have the potential to achieve these observational requirements. Based on a methodology originally proposed by *Cooney* [1972], RR lidar systems are presently operational at several scientific institutions [among others, *Behrendt and Reichardt*, 2000; *Mattis et al.*, 2002].

[4] While the methodology of the RR technique has been known for more than three decades, its effective experimental exploitation has become possible just recently because of the acquired capability to manufacture spectral selection devices with extremely high performances in terms of out-of-band rejection at the laser wavelength (10^6 or better), while guaranteeing high transmission of the RR signals ($\geq$30%). These specifications can nowadays be achieved through the use of state of the art interference filters or polychromators [*Mattis et al.*, 2002]. Their combination with Fabry-Perot interferometers allows to further reduce sky background and improve daytime performances [*Bobrovnikov et al.*, 2002].

[5] All RR lidar measurements reported in literature have been performed in the visible domain. Measurements reported in the present paper represent to our knowledge the first successful attempt to perform RR temperature measurements in the UV. The exploitation of the RR technique in the UV has the potential to achieve high precision. Additionally, UV lidars may achieve better daytime performances than visible systems due to reduced sky background. Last but not least, this spectral region is safer in terms of hazard for eye injury, with retinal damage threshold being more than 3 orders of magnitude lower than in the visible. UV laser beams used in most lidar applications result to be eye-safe within a few hundred meters from the laser source, with radiant energy density being within the limits defined by *ANSI standards* [1986].

2. Instrumental Set-Up

[6] The NASA/GSFC Scanning Raman Lidar (SRL) is a mobile system contained in a single environmentally controlled trailer [*Whiteman and Melfi*, 1999]. It includes a Nd:YAG laser, a 0.76 meter telescope and a large aperture scanning mirror. The laser source (Continuum, custom designed) is based on a 1 m length cavity and emits 350 mJ pulses at 354.7 nm, with a pulse repetition rate of 30 Hz; the laser is unseeded with linewidth of 1 cm^{-1} and frequency stability better than 0.5 cm^{-1}. Major transmitter/receiver specifications are reported in Table 1. The SRL was outfitted with a UV rotational Raman temperature measurement capability in May 2002. The filter assembly is based on the use of interference filters (IFs) manufactured by Barr. Filters' specifications, included in Table 1, were the result of a detailed sensitivity study based on a careful analysis of the temperature dependence of rotational lines. The sensitivity analysis was aimed to maximize measurement precision. In the selection of rotational lines we have to take into account that increasing the number of selected lines provides an

[1]DIFA, Università della Basilicata, Potenza, Italy.
[2]NASA/GSFC, Mesoscale Atmospheric Processes Branch, Greenbelt, Maryland, USA.

0094-8276/04/2003GL018342

Table 1. SRL Technical Specifications, as Well as Technical Specifications Considered to Simulate Performances of RR Lidar Systems at 355 and 532 nm

	SRL		532 nm system	
Nd:YAG laser				
Wavelength	355 nm		532 nm	
Single pulse energy	350 mJ		350 mJ	
Pulse repetition frequency	30 Hz		30 Hz	
Linewidth (FWHM)	1 cm^{-1}		1 cm^{-1}	
Frequency stability	0.5 cm^{-1}		0.5 cm^{-1}	
Beam divergence (full angle)	0.15 mrad		0.15 mrad	
Transmitting optics reflectivity	88%		92%	
Telescope reflectivity	88%		92%	
Telescope aperture (diameter)	0.76 m		0.76 m	
Receiver FOV	0.25 mrad		0.25 mrad	
PMTs' quantum efficiency	25%		40%	
Filter assembly for nighttime	Low-J	High-J	Low-J	High-J
CWL (nm)	354.3	352.9	531.2	528.2
FWHM (nm)	0.2	1.0	0.4	2.0
CWL transmission	30%	30%	50%	50%
Blocking @ 354.7 nm	10^{-6}	10^{-6}	10^{-6}	10^{-6}
Filter assembly for daytime	Low-J	High-J	Low-J	High-J
CWL (nm)	354.3	353.3	531.2	528.95
FWHM (nm)	0.2	0.2	0.4	0.4
CWL transmission	30%	30%	50%	50%
Blocking @ 354.7 nm	10^{-6}	10^{-6}	10^{-6}	10^{-6}

improvement of RR signals' strength, but at the same time results in a decrease of measurement sensitivity and in an increase in sky background. Consequently, the choice of the number and location of the RR lines to be selected by the filters is the result of a careful trade-off.

[7] Filters' center wavelength (CWL) can be tuned toward shorter wavelengths by increasing the angle of incident light ($\Delta\lambda \cong 0.03-0.05$ nm/deg for angles <5 deg). No thermal stabilization of the filters was needed since the effects associated with thermal drifts (0.002 nm/K) are negligible.

[8] The positions of the filters were first tuned prior to the field campaign through the use of a high spectral resolution (1.7 A) spectrometer (DigiKrom DKS 240) illuminated through a high intensity UV lamp. The positions of the filters were then optimized experimentally in the field through rotation. Figure 1 shows the calculated RR cross section vs. wavelength for N_2 and O_2 as estimated at two reference temperatures (310 and 280 K), together with transmission of interference filters in final alignment position.

[9] Photomultipliers used for the detection of RR signals were included inside unshielded housings and their performances were somewhat altered by the electromagnetic noise produced by the discharge of laser capacitors, which resulted in additional noise. In order to remove this effect, the signal discrimination level for photon counting was increased. This reduced the photon count rates in the RR signals and resulted in an unoptimized system configuration for temperature measurements.

3. Data Analysis and Results

[10] The present measurements were carried out during the International H_2O Project (IHOP), conducted in the Southern Great plains (USA) during May–June 2002. Approximately 200 hours of data were collected by the SRL and 148 radiosondes were launched during this period.

[11] Atmospheric temperature is obtained from the power ratio of high-to-low quantum number rotational Raman signals, R, through the application of the calibration function:

$$R(T) = \frac{P_{hiJ}(T)}{P_{loJ}(T)} = \exp(a/T + b) \quad (1)$$

This expression, which is exactly valid for two individual lines [*Arshinov et al.*, 1983], can be assumed to be valid also when considering portions of the RR spectrum including more rotational lines [*Behrendt and Reichardt*, 2000]. This is the case of the present measurements, with 4 rotational lines (2 from O_2, 2 from N_2) falling inside the low-J filter and 17 rotational lines (7 from O_2, 10 from N_2) falling inside the high-J filter. Calibration constants a and b in expression (1) are determined through comparison with simultaneous radiosondes. 6 lidar-radiosonde intercomparisons including both nighttime and twilight cases have been considered in this computation, leading to $a = -758 \pm 6$ and $b = -0.95 \pm 0.02$.

[12] Typical and maximum likely values for the different sources of systematic error were determined through a detailed sensitivity study. This study, based on the simulation of backscatter and background signals and the subsequent application of expression (1), allows to determine the effects on temperature retrievals of changing the instrumental parameters' values. A systematic uncertainty, with maximum and typical values of 1 K and 0.5 K, respectively, affects the estimates of a and b and it is associated with radiosonde biases (drifts of the radiosonde calibration) and with the possibility of different air masses being sensed by radiosonde and lidar. The systematic error associated with assuming the calibration function (1) to be valid for portions of the RR spectrum is found to be less than 0.8 K (typical value 0.2 K). The use of alternative analytical expressions

$$R(T) = \exp(a'/T^2 + b'/T + c'),$$

$$R(T) = \exp(a''/T^3 + b''/T^2 + c''/T + d'')$$

may lead to a systematic error less than 0.2 K. An additional source of systematic error up to 2 K below 1–2 km is

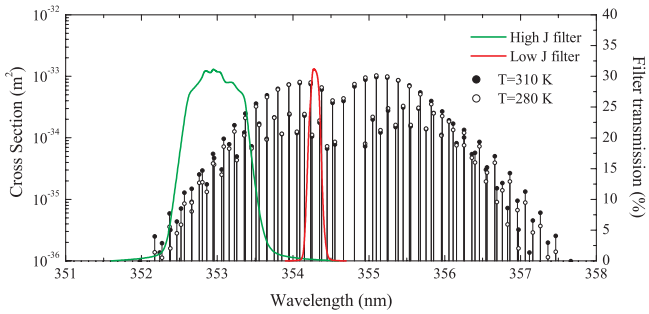

Figure 1. Calculated RR cross section versus wavelength for N_2 and O_2 as estimated at 310 and 280 K, together with transmission of interference filters in final alignment position.

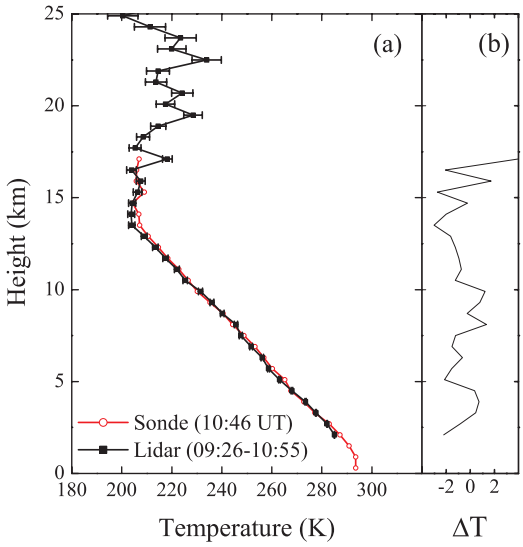

Figure 2. (a) Temperature profile on June 9, 2002 (nighttime conditions): lidar measurement (black solid line) and radiosonde data (red solid line); (b) Deviations between lidar and radiosonde.

associated with slight receiver misalignment leading to different overlap functions in the two RR channels. This error source can be reduced by fiber coupling the receiver exit, exploiting optical fibers' property to homogenize the *f* number of the transmitted radiation [*Arshinov et al.*, 2003]. Laser frequency fluctuations resulting from thermal drifts inside the laser cavity (0.1 cm^{-1}/K) can lead to a maximum systematic error of 0.5 K (typical value = 0.1 K). Assuming the different sources of systematic error to be independent, the maximum overall systematic error is smaller than 2.4 K below 2 km and smaller than 1.3 K above, while a typical value is 0.5 K.

[13] Lidar data, acquired with a vertical resolution of 30 m, have been vertically smoothed to a final resolution of 600 m in order to reduce signal statistical fluctuations. Smoothing procedure is based on data binning, assigning equal weight to each data point.

[14] Figure 2a shows a lidar measurement of the temperature profile carried out on June 9, 2002 (09:26–10:55 GMT) and the simultaneous temperature profile measured by radiosonde (Vaisala, RS80, launch at 10:46 GMT). Error bars in the figure include statistical uncertainty only, which is obtained through error propagation considering Poisson statistics for both backscatter and background signals. The reported lidar measurement, carried out in almost clear sky conditions, ended half hour before sunrise. The lidar measurement extends up to approximately 23 km (height where the random error gets larger than 5 K), with random error being 1.5 K at 15 km. Lidar and radiosonde measurements appear to be in good agreement, with deviations between the two sensors (Figure 2b) being less than 3 K up to approx. 17 km (max. height for radiosonde) and less than 2 K up to 14 km, with an average bias up to 12 km of 0.5 K and a RMS deviation of 1.2 K. It is to be pointed out that the present lidar temperature measurement, as well as the one in Figure 3, was not used for the determination of the calibration coefficients, so that this measurement results to be completely independent from simultaneous radiosonde data.

[15] Figure 3a shows the temperature profile measurement for June 2, 2002. The lidar measurement (01:00–02:30 GMT), started one hour before sunset (twilight conditions) in almost clear sky (radiosonde launch at 02:40 GMT). In this case lidar measurements extend up to approximately 14 km. Note that the smaller vertical range covered by this measurement with respect to the previous is the result of the fact that the present measurement was performed in day-dusk transition, when lidar performances are degraded by the presence of solar background noise. The deviations (Figure 3b) between lidar and radiosonde data for this measurement do not exceed 3 K, with an average bias up to 12 km of 0.2 K and a RMS deviation of 1.8 K. Once again, RMS deviations are somewhat larger than those observed on June 9 as a result of the larger statistical uncertainty affecting daytime versus nighttime lidar measurements.

[16] Results discussed in this paper, although accomplished with an unoptimized lidar system, clearly show that the application of the RR technique in the UV allows high quality measurements of the temperature profile throughout the troposphere. Simulations have been performed in order to quantify the potential of the technique in terms of measurement precision at 355 and 532 nm, for both nighttime and daytime operation, through the expression [*Behrendt and Reichardt*, 2000]:

$$\Delta T(z) = \frac{\partial T(z)}{\partial R} R(z) \sqrt{\frac{P_{loJ}(z) + bk_{loJ}}{P^2_{loJ}(z)} + \frac{P_{hiJ}(z) + bk_{hiJ}}{P^2_{hiJ}(z)}} \quad (2)$$

assuming Poisson statistics for both backscatter and background signals. The term $bk_{loJ/hiJ}$ represents the sky background signal. Up to 2 μm, daylight background is mainly determined by scattering of sunlight. Daylight background (sun zenith angle = 40°) was simulated considering molecular scattering only. It is to be pointed

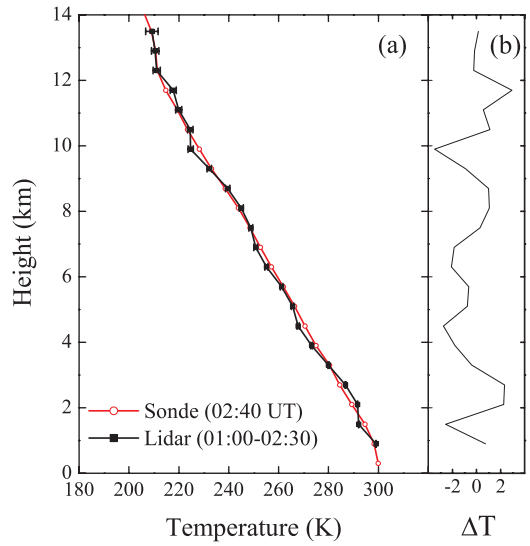

Figure 3. (a) Temperature profile on June 2, 2002 (twilight conditions): lidar measurement (black solid line) and radiosonde data (red solid line); (b) Deviations between lidar and radiosonde.

out that extraterrestrial solar irradiance around 355 nm is approx. 5 times smaller than at 532 nm. In order to compute backscatter signals, we considered vertical profiles of pressure, temperature and humidity taken from US standard atmosphere (1976). Aerosol extinction data were taken from the ESA ARMA median model. Attenuation due to cloud extinction may significantly reduce signal strength: however, cloud extinction was not considered in the present clear sky simulations. While measurements can penetrate clouds with small optical thickness, nevertheless particular care has to be paid on the manufacturing of the filters in order to guarantee rejection of Rayleigh/Mie signals. A filter blocking at the laser wavelength of 10^{-6} has been estimated to prevent from contamination due to elastic echoes from aerosol/cloud structures with scattering ratios up to 10.

[17] System parameters considered for the simulation at 355 nm are those of SRL (Table 1). System parameters considered at 532 nm (also in Table 1) have been defined based on state-of-the art specifications of lidar systems at this wavelength. In order to properly compare performances at 355 and 532 nm, the approximate power-aperture product of the SRL (5 Wm^2) was considered at each wavelength. Additionally, filters' specifications considered for nighttime operation at 532 nm were defined in order to isolate the same rotational Raman lines as at 355 nm (same quantum numbers). Such RR lines selection was verified to guarantee best precision, as at 355 nm. Filters' specifications at 532 nm result very close to those defined by *Behrendt and Reichardt* [2000] and have been verified to be feasible by Barr.

[18] Daytime simulations consider two distinct spectral selection configurations: one based on the use of IFs only (configuration 1), the second based on the combination of a Fabry-Perot (FP) interferometer and IFs (configuration 2). This second configuration, applicable only in case of use of a seeded laser, reduces sky background, consequently improving daytime performances [*Bobrovnikov et al.*, 2002]. Potential gain in signal-to-background ratio is approx. a factor of 65 (ratio between the average separation between adjacent lines, 3.3 cm^{-1}, and the spectral width of individual lines, 0.5 cm^{-1}). FB transmission is assumed to be 60% and its finesse is taken equal to 20.

[19] The optimization of filters' specifications for daytime operation required a separate sensitivity study, accounting for the wavelength variability of daytime background radiation and leading to the selection of a different set of RR lines, as compared to nighttime operation. IFs specifications for configuration 1 are reported in Table 1, while IFs specifications for configuration 2, being very close to those of configuration 1, are ignored in the table.

[20] Figure 4 shows the simulated measurement precision, ΔT, versus height at 355 and 532 nm, both for nightime and daytime operation. The lower scale represents ΔT for 1 hour time integration, while the upper scale represents ΔT for 15 minute time integration. To fit the WMO requirements given in the introduction, a vertical resolution of 100 m was considered in the simulations. For nighttime operation, ΔT_{355} and ΔT_{532} are comparable up to 8 km, while above this height ΔT_{355} gets worse (up to 30%) than ΔT_{532}. For nighttime operation and 1 hour integration,

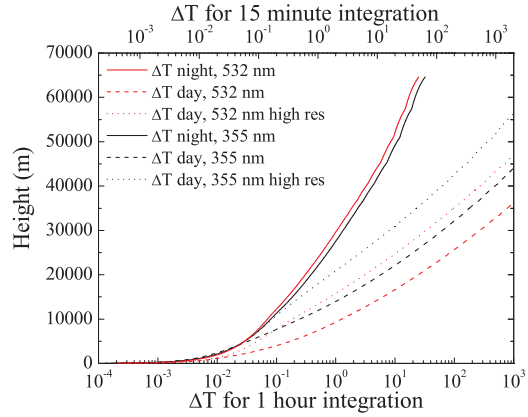

Figure 4. ΔT_{355} (black line) and ΔT_{532} (red line), for both nigh-time (solid line) and daytime operation (dashed line for IF based spectral selection assembly and dotted line for Fabry-Perot interferometer + IFs assembly).

ΔT is found to not exceed 0.2 K up to 15 km at both 355 and 532 nm. This uncertainty is approximately 5 times smaller than the one characterizing nighttime measurements during IHOP (Figure 2a), as a result of the non-optimized system configuration mentioned earlier. For nighttime operation and 15 minute integration, ΔT is found to not exceed 0.5 K up to 15 km at both 355 and 532 nm, which satisfies WMO observational requirements for climate and meteorological applications indicated in the introduction.

[21] Simulations of daytime performances reveal that, in case of use of IF based spectral selection assembly, ΔT_{355} is up to a factor of 4 better than ΔT_{532}, with ΔT_{355} not exceeding 1.5 K throughout the troposphere for 1 hour integration. In case of use of state of the art Fabry-Perot interferometer + IFs assembly, ΔT is up to 7 times better than that obtained with the IF based spectral selection assembly at both 355 and 532 nm, and ΔT_{355} is up to a factor of 4 better than ΔT_{532}, with ΔT_{355} not exceeding 0.3 K throughout the troposphere for 1 hour integration.

4. Summary

[22] Atmospheric temperature measurements in the UV spectral region have been performed through the application of the pure rotational Raman technique. Nighttime measurements are found to extend up to 23 km, with a vertical resolution of 600 m and a time resolution of 90 minutes. RMS deviation between lidar and simultaneous radiosondes does not exceed 1.2 K and average bias is not exceeding 0.5 K. In order to suppress undesired electronic noise induced by the laser, the acquisition system was slightly modified, resulting in an unoptimized system configuration and leading to averaging times inadequate for meteorological applications. However, simulations show that, based on 15 minute time integration, the use of an optimized system including state of the art transmitters and receivers may allow nighttime temperature measurements throughout the troposphere with errors not exceeding 0.5 K at both 355 and 532 nm, which would permit WMO observational requirements for climate and meteorological applications to be fulfilled. Simulations also reveal that the application of the RR technique at UV wavelengths has strong potential for

daytime measurements. The methodology presented here has the advantage of possessing greatly reduced eye hazard, thus allowing for the implementation in operational continuously monitoring lidar stations.

[23] **Acknowledgments.** This research was sponsored by NASA's program for Interdisciplinary studies headed by Dr. J. Dodge and by the National Science Foundation.

References

ANSI (1986), American national standard for the safe use of lasers, *Am. Nat. Stand. Inst.,* Z136. 1–1986, New York.

Arshinov, Y. F., S. M. Bobrovnikov, V. E. Zuev, and V. M. Mitev (1983), Atmospheric temperature measurements using pure rotational Raman lidar, *Appl. Opt.*, *22*, 2984–2990.

Arshinov, Y. F., D. Althausen, A. Ansmann, S. Bobrovnikov, I. Mattis, D. Müller, I. Serikov, and U. Wandinger (2003), Round-the-clock temperatur profiling in the troposphere with Raman lidar, *ISTP 2003, Extended Abstracts*, 142–144.

Behrendt, A., and J. Reichardt (2000), Atmospheric temperature profiling in the presence of clouds with a pure rotational Raman lidar by use of an interference-filter-based polychromator, *Appl. Opt.*, *39*, 1372–1378.

Bobrovnikov, S., Y. F. Arshinov, and I. B. Serikov (2002), Daytime temperature profiling in the troposphere with a pure rotational Raman lidar, 21st ILRC, Quebec, *Proceedings, Part II*, 717–720.

CEOS/WMO Online Database (2003), Version 2.5, Observational requirements, http://alto-stratus.wmo.ch/sat/stations/_asp_htx_idc/Requirements.asp.

Cooney, J. A. (1972), Measurements of atmospheric temperature profiles by Raman backscatter, *J. Appl. Meteorol.*, *11*, 108–112.

Mattis, I., A. Ansmann, D. Althausen, V. Jaenisch, U. Wandinger, D. Müller, Y. F. Arshinov, S. M. Bobrovnikov, and I. B. Serikov (2002), Relative-Humidity Profiling in the Troposphere with a Raman Lidar, *Appl. Opt.*, *41*, 6451–6462.

Whiteman, D. N., and S. H. Melfi (1999), Cloud liquid water, mean droplet radius and number density measurements using a Raman lidar, *J. Geophys. Res.*, *104*, 31,411–31,419.

World Meteorological Organization (1996), Commission on Basic Systems (CBS) Working Group on Satellites, Final Report.

P. Di Girolamo and R. Marchese, DIFA, Università della Basilicata, Potenza, Italy. (digirolamo@unibas.it)

D. N. Whiteman and B. B. Demoz, NASA/GSFC, Mesoscale Atmospheric Processes Branch, Greenbelt, MD, USA.